Efficiency and robustness of coherent population transfer with intense, chirped laser pulses

Vladimir S. Malinovsky and Jeffrey L. Krause
Quantum Theory Project, University of Florida, P.O. Box 118435, Gainesville, Florida 32611-8435
(Received 15 May 2000; published 20 March 2001)

We discuss electronic population transfer in diatomic molecules. By analyzing time-dependent wave packets on electronic potential-energy surfaces, we investigate the efficiency and robustness of population transfer with intense, chirped laser pulses. Recently, the magnitude of the population transfer was observed to have a remarkable dependence on the sign of the chirp [J. Cao, C. J. Bardeen, and K. R. Wilson, Phys. Rev. Lett. **80**, 1406 (1998)]. In this work we explain the reason for this asymmetry, and show how the frequency detuning, intensity, and chirp rate affect the results. In particular, we demonstrate efficient, robust population transfer for both positive and negative chirps. A Landau-Zener model of multiple avoided crossings is invoked to model the results.

DOI: 10.1103/PhysRevA.63.043415 PACS number(s): 42.50.Hz, 32.80.Qk, 33.80.Be

I. INTRODUCTION

A variety of methods, both experimental and theoretical, have been implemented to achieve population transfer in atomic and molecular systems [1–7]. Efficient, robust schemes to invert population selectively have applications in a number of areas, such as improved lasing efficiency [8], induced transparency [9,10], preparation of initial states for spectroscopy [1,5,7], Bose-Einstein condensates [11], and quantum control [12–17]. In this paper, we concentrate on electronic population transfer in diatomic molecules, using ultrafast, chirped laser pulses. We investigate the effects of intensity, chirp rate, and frequency detuning using a dressed-state picture to determine the optimal conditions for vibronic population inversion.

Population transfer in two-level systems is now well understood [18,19]. Several different strategies to do this have been demonstrated in experiments. In one, the center frequency is resonant with the transition frequency, and the pulse area (the integral of the pulse) is set to π. This scheme, which is used commonly in magnetic resonance, for example [20,21], can achieve 100% population transfer. The results are not sensitive to the detailed shape of the pulse, but are extremely sensitive to the area. This can lead to experimental difficulties in implementing such methods, particularly in the ultrafast regime.

Population transfer by adiabatic passage [1,2] is a more robust scheme than the use of π pulses with respect to the pulse parameters. In chirped adiabatic passage, the laser frequency is tuned below (or above) the transition frequency, and the frequency chirp is swept through resonance. Alternatively, the laser pulse can be transform limited (zero chirp), and a Stark switching technique can be used to sweep the transition frequency through resonance [1,22]. In both cases, as long as the process is performed adiabatically, the desired final state can be populated with 100% efficiency.

Electronic population transfer in molecules is in general much more complicated than atomic or magnetic two- (or *n*-) level systems. In the ultrafast regime, the bandwidth of the excitation laser creates a coherent superposition of many vibrational states on the excited potential surface. It is practically impossible to satisfy the resonance and area conditions for all of these transitions simultaneously. Thus, in the commonly used sense of the term, no ultrafast π pulse is possible for a molecular system. However, all is not lost. Numerous theoretical schemes using chirped adiabatic passage have been proposed for molecules [3,23–25], and rotational population transfer has now been observed experimentally [7,26–29].

Recently, Cao, Bardeen, and Wilson (CBW) suggested a general method for population transfer in molecules [30]. Their method, which they termed the molecular ''π pulse,'' requires a pulse with a large bandwidth, a high intensity, and a large positive chirp. They noted a strong dependence on the sign of the chirp, both with respect to the efficiency of population transfer and the robustness of the results to small changes in the magnitude of the chirp. Their explanation for the mechanism of such pulses is based on the classical idea that the wave packet is created initially with the low-frequency components of the pulse, which are on resonance with the desired transition frequency. As the wave packet evolves on the excited state, the high-frequency components of the pulse become off-resonant, and the population is trapped on the excited state. CBW find that their results are robust to changes in the laser parameters, and suggest that this method may be quite general. Experiments have now verified their predictions on systems ranging from molecular iodine to laser dyes and green fluorescent protein [31–33].

In this paper, we analyze the results of CBW in a dressed-state picture using a Landau-Zener model. We analyze the dependence of the results on intensity and frequency detuning and find that, depending on the sign of the detuning, a negatively chirped pulse can be as effective as a positively chirped pulse. The dressed-state picture enables simple predictions of the optimal conditions for population transfer.

II. THEORY

In this work we concentrate on electronic population transfer in diatomic molecules. The theory for this situation is well developed. In this section we sketch the formalism briefly to define the parameters and specify the model clearly.

The theory proceeds by integrating the time-dependent Schrödinger equation for the coupled electronic states on a numerical grid using a split-operator method. The general form of the dynamical equations is

$$i\hbar\frac{\partial}{\partial t}\begin{pmatrix}\psi_1(t)\\ \psi_2(t)\end{pmatrix}=\begin{pmatrix}T+V_1 & -W\\ -W & T+V_2\end{pmatrix}\begin{pmatrix}\psi_1(t)\\ \psi_2(t)\end{pmatrix}, \tag{1}$$

where

$$T=-\frac{\hbar^2}{2m}\frac{\partial^2}{\partial x^2} \tag{2}$$

is the kinetic operator, m is the reduced mass, V_i ($i=1$ and 2) are the electronic potential-energy surfaces, and

$$W=E_0S(t)\mu_{12}(x)\cos(\varphi(t)) \tag{3}$$

is the coupling operator. In this equation, μ_{12} is the dipole moment and the laser field is described by a pulse envelope $S(t)$, peak amplitude E_0, and time-dependent phase $\varphi(t)$.

A short-time evolution operator is used in the form [34]

$$\exp\left[-\frac{i\Delta t}{\hbar}\begin{pmatrix}T+V_1 & -W\\ -W & T+V_2\end{pmatrix}\right]$$
$$=\exp\left[-\frac{i\Delta t}{2\hbar}\begin{pmatrix}V_1 & -W\\ -W & V_2\end{pmatrix}\right]\exp\left[-\frac{i\Delta t}{\hbar}\begin{pmatrix}T & 0\\ 0 & T\end{pmatrix}\right]$$
$$\times\exp\left[-\frac{i\Delta t}{2\hbar}\begin{pmatrix}V_1 & -W\\ -W & V_2\end{pmatrix}\right]+O(\Delta t)^3. \tag{4}$$

We use a fast Fourier transform to convert between the coordinate space and momentum space representations, which allows a facile evaluation of the kinetic-energy terms. By using unitary transformation, it is straightforward to show that

$$\exp\left[-\frac{i\Delta t}{2\hbar}\begin{pmatrix}V_1 & -W\\ -W & V_2\end{pmatrix}\right]=\exp\left(-i\frac{\Delta t(V_1+V_2)}{4\hbar}\right)\begin{pmatrix}\cos\beta+i\frac{\Delta t(V_2-V_1)}{4D}\sin\beta & i\frac{2W}{D}\sin\beta\\ i\frac{2W}{D}\sin\beta & \cos\beta-i\frac{\Delta t(V_2-V_1)}{4D}\sin\beta\end{pmatrix}, \tag{5}$$

where $\beta=\Delta tD/4\hbar$ and $D^2=(V_2-V_1)^2+4W^2$. Using Eq. (5) allows the method to proceed without numerical diagonalization of the potential-energy matrices [35].

The time-dependent phase of the laser pulse, $\varphi(t)$, is expanded in a Taylor series. Our interest in this work is the effect of the linear chirp, so the series is truncated after three terms,

$$\varphi(t)=\varphi_0+\omega_0t+\tfrac{1}{2}\alpha t^2, \tag{6}$$

where φ_0 is an irrelevant phase constant, ω_0 is the center frequency, and α is the temporal linear chirp.

Using Eq. (6) and applying the rotating wave approximation (RWA) the Hamiltonian in Eq. (1) takes the form

$$H(t)=\begin{pmatrix}T+U_1 & -\Omega_0S(t)/2\\ -\Omega_0S(t)/2 & T+U_2\end{pmatrix}, \tag{7}$$

where $U_1=V_1$, $U_2=V_2-\hbar(\omega_0+\alpha t)$, and $\Omega_0=E_0\mu_{12}(x)$ is the peak Rabi frequency. Below we present results obtained in the RWA using the evolution operator in Eq. (5) with the simple transformations

$$V_1\rightarrow U_1, V_2\rightarrow U_2 \tag{8}$$

and

$$W\rightarrow\Omega_0S(t)/2. \tag{9}$$

III. CHARACTERISTICS OF CHIRPED LASER PULSES

We consider a Gaussian functional form for the laser pulse,

$$E(t)=E_0\exp\left[-\frac{t^2}{2\tau^2}-i\omega_0t-i\alpha\frac{t^2}{2}\right], \tag{10}$$

where τ is pulse duration, ω_0 is the center frequency, α is the temporal linear chirp, and E_0 is the peak amplitude. The Fourier transform of Eq. (10) gives the field in the frequency domain,

$$E(\omega)=E_0'\exp\left[-\frac{(\omega-\omega_0)^2}{2\Gamma^2}+i\alpha'\frac{(\omega-\omega_0)^2}{2}\right], \tag{11}$$

where Γ is the bandwidth of the pulse and α' is the spectral linear chirp. Note that the full width at half maximum (FWHM) duration of the pulse is $\tau_{\mathrm{FWHM}}=\tau\sqrt{\ln 16}$, and the FWHM of the bandwidth is $\Gamma_{\mathrm{FWHM}}=\Gamma\sqrt{\ln 16}$. For simplicity we suppress these numerical constants in the following discussion.

The relations between the pulse duration and the bandwidth are

$$\Gamma^2=\frac{1}{\tau^2}(1+\alpha^2\tau^4) \tag{12}$$

and

$$\tau^2=\frac{1}{\Gamma^2}(1+\alpha'^2\Gamma^4). \tag{13}$$

The relations between the temporal and spectral chirp rates are

$$\alpha'=\alpha\frac{\tau^4}{(1+\alpha^2\tau^4)} \tag{14}$$

and

$$\alpha=\alpha'\frac{\Gamma^4}{(1+\alpha'^2\Gamma^4)}. \tag{15}$$

Equations (12) and (14) are valid for the case of fixed pulse duration, τ, while Eqs. (13) and (15) are valid for the case of a fixed bandwidth Γ.

Chirping a laser pulse reduces its peak intensity. To conserve the integrated intensity $P_0=E_0^2\tau$ for a given bandwidth Γ, the intensity of a chirped pulse is

$$I=I_0\frac{1}{\sqrt{1+\alpha'^2\Gamma^4}}. \tag{16}$$

In this equation, I_0 is the peak intensity of the transform-limited pulse, and $\Gamma=1/\tau_0$ is the bandwidth of the transform-limited pulse with duration τ_0.

Figure 1 illustrates how the intensity I, pulse duration τ, and temporal chirp α depend on the spectral chirp α' at a fixed bandwidth Γ. In this figure, the duration of the transform-limited pulse is $\tau_0=13.55$ fs. This figure illustrates concisely several features of chirped laser pulses that will be important in the following discussion. Note, first, that while the range of α' is unlimited (that is, α' can take any value from $-\infty$ to ∞), the range of α is finite (for a fixed bandwidth, with the chirp produced via linear optics). It is simple to show that the maximum value of α is related to the transform-limited pulse duration and bandwidth by

$$\alpha_{\max}=\frac{\Gamma}{2\tau_0}. \tag{17}$$

This relation implies that the maximum amount that a pulse can be stretched in the time domain by using a temporal frequency chirp is $\tau_{\max}=\tau_0\sqrt{2}$. However, with a spectral chirp, a pulse can, in principle, be stretched infinitely long. This is, of course, the principle behind the chirped pulse amplifier now in common use [36]. Note, too, that the region in which α changes rapidly corresponds to the region in which the pulse duration and intensity are changing slowly. It is clear, in this figure, that to derive the maximum physical effect from the chirp, the value of α' will, in general, correspond to the relatively narrow range in which α is changing rapidly. Finally, as we demonstrated previously [37], although it is possible mathematically, and is sometimes desirable, to use values of α larger than $\alpha_{\max}$, this results in a pulse with a laser bandwidth larger than the initial, transform-limited pulse. This is impossible with linear optics.

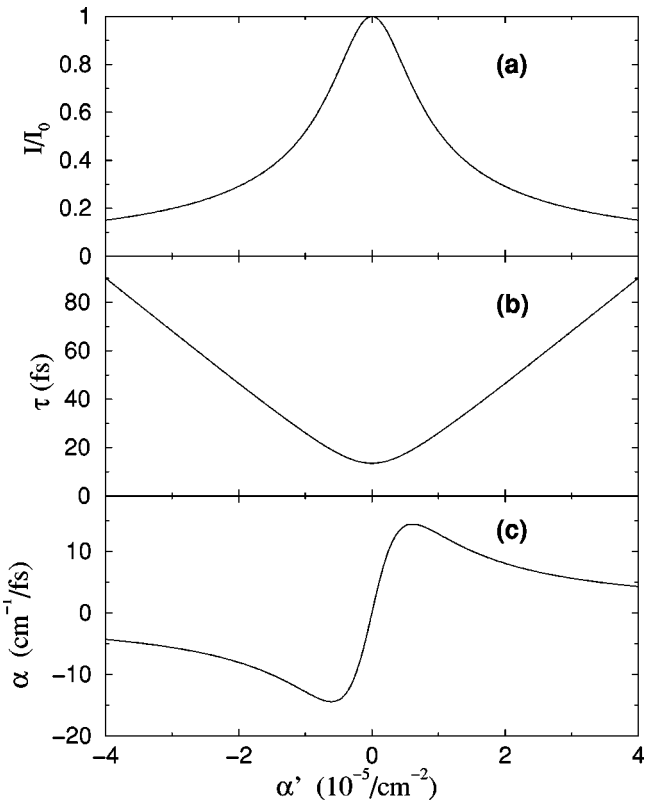

FIG. 1. Dependence of the scaled intensity I/I_0, duration, τ, and temporal linear chirp α on the spectral linear chirp α' for a pulse with fixed bandwidth Γ. The duration of the transform-limited pulse τ_0 is 13.55 fs.

IV. POPULATION TRANSFER

A. Numerical results

As a specific example of population transfer, consider the iodine molecule, as depicted schematically in Fig. 2. The molecule begins in the $v=0$ vibrational level on the ground X electronic state. An ultrafast laser pulse creates a wave packet composed of vibrational levels on the electronically excited B state. For simplicity, we invoke the Condon approximation and neglect the position dependence of the $B\leftarrow X$ transition dipole moment. That is, we assume that μ_{12} is a constant. Our goal is to determine under what conditions the population transfer to the B state is maximized.

Figure 3 shows the population transfer to the B state at asymptotic times (i.e., after the pulse is over) as a function of the peak Rabi frequency, Ω_0, and spectral linear chirp, α'. In this figure, the laser pulse has a constant bandwidth corresponding to a transform-limited pulse duration of 13.55 fs, and the center frequency is chosen to be on-resonance with the vertical transition energy. Under these conditions, as can be seen in the figure, negatively chirped pulses are distinctly less effective at population transfer than positively chirped pulses. For negative chirps, some ''islands'' of moderate

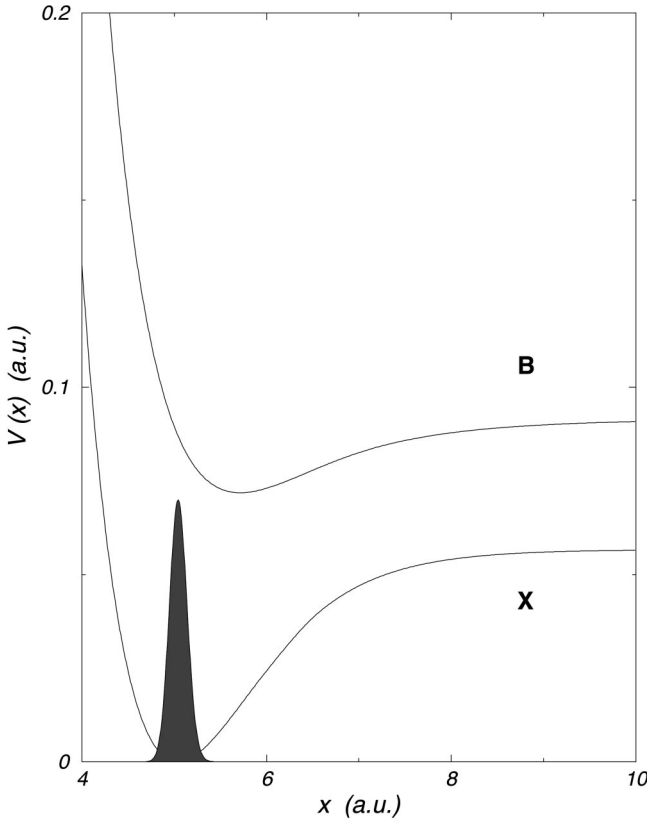

FIG. 2. Electronic potential energy surfaces for I_2, after Ref. [42].

($\geqslant 60\%$) population transfer exist, but for positive chirps there are large areas of nearly total population transfer. The results in Fig. 3, showing robust population transfer for positive chirps, and comparatively poor population transfer for negative chirps, are identical to those presented previously by CBW [30].

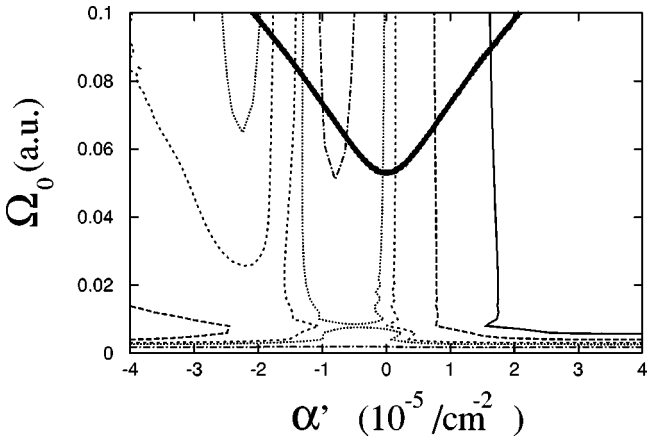

FIG. 3. Population transfer as a function of the peak Rabi frequency, Ω_0, and the spectral linear chirp, α'. The center frequency of the laser is on resonance with the vertical transition energy, and the transform-limited pulse width is 13.55 fs. The isolines in the plot represent final yields of 0.98 (solid line), 0.90 (long dashed line), 0.70 (dashed line), 0.60 (dotted line), and 0.40 (dot-dashed line). The *y* axis labels the peak Rabi frequency of the transform-limited pulse. The thick solid line demarks the region of peak intensities of 1×10^{14} W/cm^2.

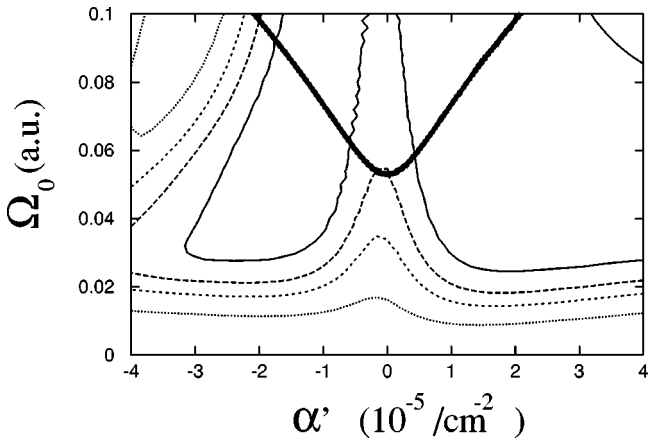

FIG. 4. Population transfer as a function of the peak Rabi frequency, Ω_0, and spectral linear chirp, α'. The detuning of the center frequency ω_0 from the vertical transition energy is equal to -0.012 a.u. (2634 cm^{-1}), and the transform-limited pulse width is 13.55 fs. The isolines in the plot represent final yields of 0.98 (solid line), 0.80 (long dashed line), 0.50 (dashed line), and 0.10 (dot-dashed line). The *y* axis labels the peak Rabi frequency of the transform-limited pulse. The thick solid line demarks the region of peak intensities of 1×10^{14} W/cm^2.

To investigate the sensitivity of the results to the laser center frequency, we repeated the calculations of Fig. 3 with a frequency detuning (from the resonance condition) of -0.012 a.u. (2634 cm^{-1}). As seen in Fig. 4, the detuning changes the results significantly. Large areas of nearly complete population transfer exist for both positive and negative chirps. Note also that as the peak Rabi frequency approaches 0.1 a.u., chirped pulses offer no advantage compared to a transform-limited pulse. However, for smaller Rabi frequencies, using either a positive chirp or a negative chirp increases the transfer efficiency significantly.

As a way of analyzing the robustness of the population transfer with respect to the center frequency, we choose a fixed Rabi frequency of $\Omega_0=0.1$ a.u., and vary the detuning and the chirp rate (while holding the bandwidth constant). The results are shown in Fig. 5. Note, in the figure, the large area of efficient population transfer for positive chirps, and the smaller area of efficient transfer for negative chirps. While positive chirps are clearly more robust, at a chirp rate of -1×10^{-5}/cm^{-2}, for example, the center frequency can be varied by as much as 0.006 a.u. (1317 cm^{-1}) while maintaining a population transfer of $>98\%$. Note also that large positive detunings tend to favor large positive chirps. It is clear, in this figure, that experimental studies of population transfer can employ either positive or negative chirps, depending on the Rabi frequency and detuning.

One factor that must be considered when analyzing results such as those in Figs. 3–5 is ionization. If the ionization rate is high enough, the molecule will not experience the intensities required for efficient population transfer. A simple estimate based on Ammosov, Delone and Krainov (ADK) [38] or Keldysh [39] theory for I_2 indicates that ionization becomes a dominant factor at intensities above 1

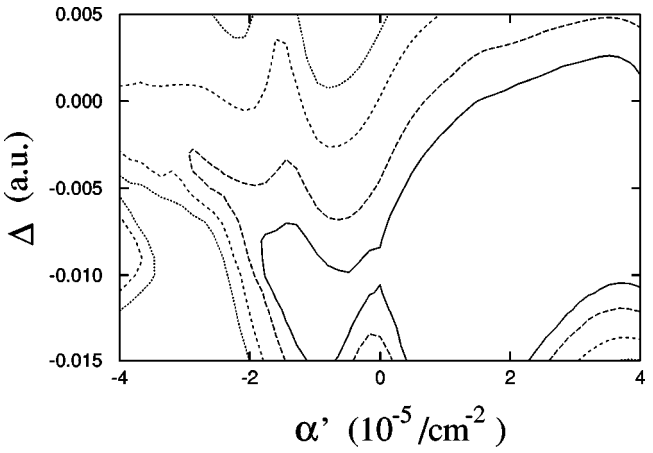

FIG. 5. Population transfer as a function of the detuning, Δ, of the center frequency ω_0 from the frequency of the vertical transition energy, and the spectral linear chirp α'. The peak Rabi frequency is 0.1 a.u., and the transform-limited pulse width is 13.55 fs. The isolines in the plot represent final yields of 0.98 (solid line), 0.90 (long dashed line), 0.60 (dashed line), and 0.3 (dotted line).

$\times 10^{14}$ W/cm^2 (a peak Rabi frequency of 0.05 a.u.). Figures 3 and 4 show the boundary corresponding to peak intensities of 1×10^{14} W/cm^2. Our estimate based on ADK theory shows that 50% of the molecules will be ionized by a transform-limited pulse with a width of $\tau_0=13.55$ fs, and an intensity of 1×10^{14} W/cm^2. However, chirping the pulse reduces the peak intensity, which allows a larger fraction of the molecules to survive. For example, with a chirp of $\alpha'=5\times\tau_0^2\approx3\times10^{-5}$/cm^{-2}, 95% of the molecules survive. With higher chirp rates, all of the molecules survive. Clearly, large areas of parameter space exist below the limiting curves in Figs. 3–4 in which the mechanism suggested here is valid.

B. Theoretical analysis of results

The asymmetry in the dependence of the final-state population on the sign of the chirp can be understood easily by considering a dressed-state picture. In this model, the vibrational levels on the ground state, dressed by the laser field, undergo a series of avoided crossings with the vibrational levels on the excited state. The degree to which the population passes through these regions determines the magnitude of the population transfer. As an example, two cases (positive and negative chirp) are shown in Fig. 6. In this figure, X_i and B_i represent vibrational levels in the X and B manifolds, respectively. Diabatic states are represented by solid lines, and adiabatic states by dashed lines. As can be seen in the figure, a clear difference exists between the dynamics of vibrational level populations for positive chirps [Fig. 6(a)] and negative chirps [Fig. 6(b)].

In Fig. 6, the population is initially in X_0, the $v=0$ level on the X state. As the pulse proceeds in time (left to right in the figure), the vibrational manifold of the excited state, B, slopes down (up) as a result of the positive (negative) chirp. Many crossings and avoided crossings (some of them indicated by a, b, and c in the figure) appear as a result of the

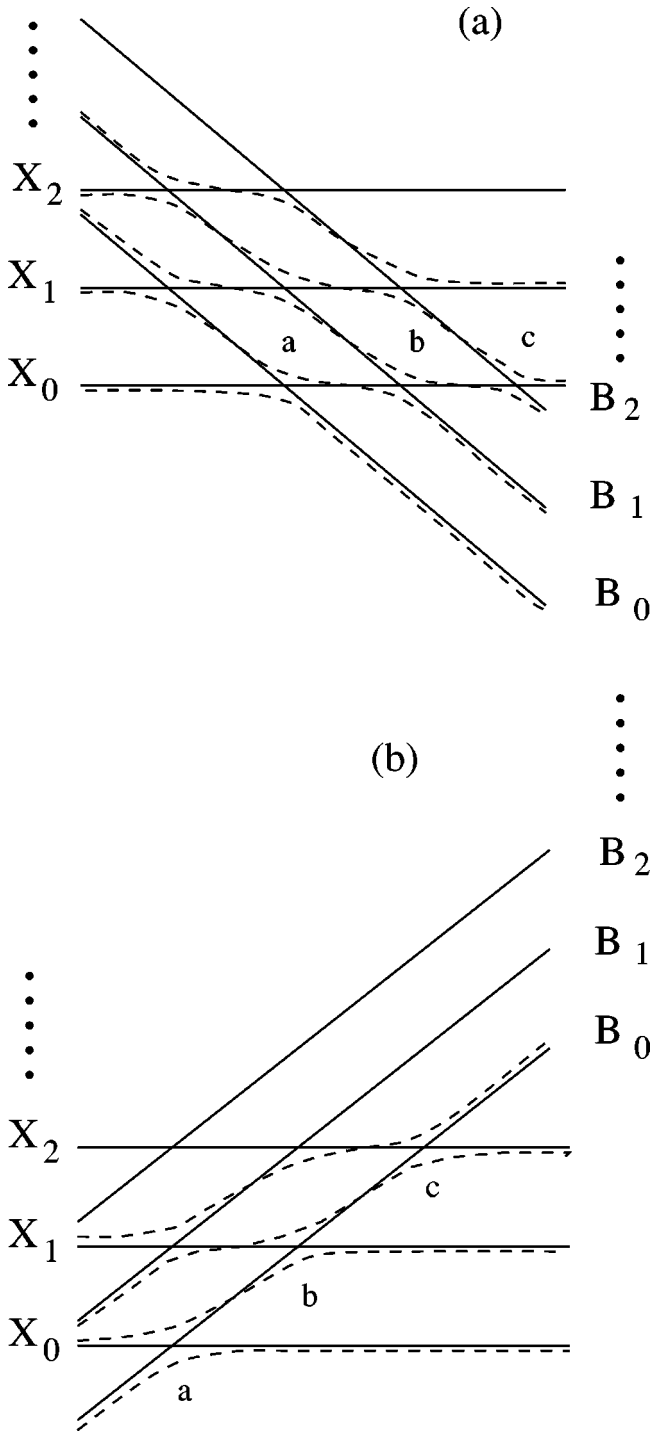

FIG. 6. Schematic of multiple crossings of vibrational levels of the electronic potentials X and B of I_2. The solid lines represent diabatic states, and the dashed lines represent adiabatic states. Panel (a) illustrates the effect of a positive chirp, and panel (b) the effect of a negative chirp. The symbols *a*, *b*, and *c* label representative crossing points.

laser frequency sweeping through resonance in the presence of the light-induced coupling. For appropriate values of the intensity and temporal chirp rate, all crossings of the diabatic curves (solid lines) can be considered independently. In this case partial population transfer by adiabatic rapid passage

occurs at the time of each crossing. However, the population for positive and negative chirps follows different routes. In the case of the positive chirp, the population is transfered sequentially to the vibrational levels B_0, B_1, B_2, etc. The amount of transfer to each level can be determined using the Landau-Zener formula [40,41]

$$P_{i\to j}=P_i-\exp\left(-\pi\frac{\Omega_{ij}^2(t_i)}{2\alpha}\right), \tag{18}$$

where P_i is the population before the avoided crossing, $\Omega_{ij}(t_i)$ is the Rabi frequency (assumed to be constant during the transition) at the time of crossing, and α is the temporal linear chirp.

By applying this consideration to each crossing we can see that for a sufficiently long pulse and properly chosen Rabi frequency all of the population from the X manifold can be transferred to the B manifold for a positive chirp. The same is not necessarily true for the negative chirp. In this case, the route to population transfer is more complicated, and less direct. As can be seen in the figure, population transferred to the B state at early times can transfer back to the higher vibrational levels of the X manifold [crossings labeled a, b, and c in Fig. 6(b)] at later times. It is clear that only under special circumstances can the entire population be transferred to the B state with a negative chirp, and remain there after the laser pulse is over.

For the scenario discussed above to be valid, several relations among the pulse parameters and vibrational energy spacing must be satisfied. To allow the possibility of several crossings during the pulse, the vibrational spacings $\delta_{X,B}$ and temporal chirp rate must obey the relation

$$\alpha\tau > \delta_{X,B}, \tag{19}$$

where τ is the duration of the chirped pulse. To maintain adiabaticity, and to apply the Landau-Zener model, the following inequality must be satisfied:

$$\delta_{X,B} > \Omega_0 \geqslant \sqrt{\alpha}. \tag{20}$$

If Eqs. (19) and (20), are obeyed, successful population transfer can be achieved with either a positive chirp or a negative chirp.

The scenario presented above has several limiting cases, depending on whether or not the relations in Eqs. (19) and (20) are satisfied. First, if Eq. (20) is obeyed, but Eq. (19) is not, the system is effectively a two-level system, and only one crossing of two diabatic states occurs. By choosing a proper detuning, a simple avoided crossing exists in the adiabatic representation, and successful population transfer is possible for either positive or negative chirps. In this case population transfer is also selective. That is, the transfer occurs from a single initial state to a single final state.

Another limiting case results is the situation in which the Rabi frequency is large compared to the vibrational energy-level spacing. In this case, the simple dressed-state picture of individual crossings must be revised. The various vibrational states have quite different shifts due to the varying Frank-Condon factors and detunings from resonance. This results in

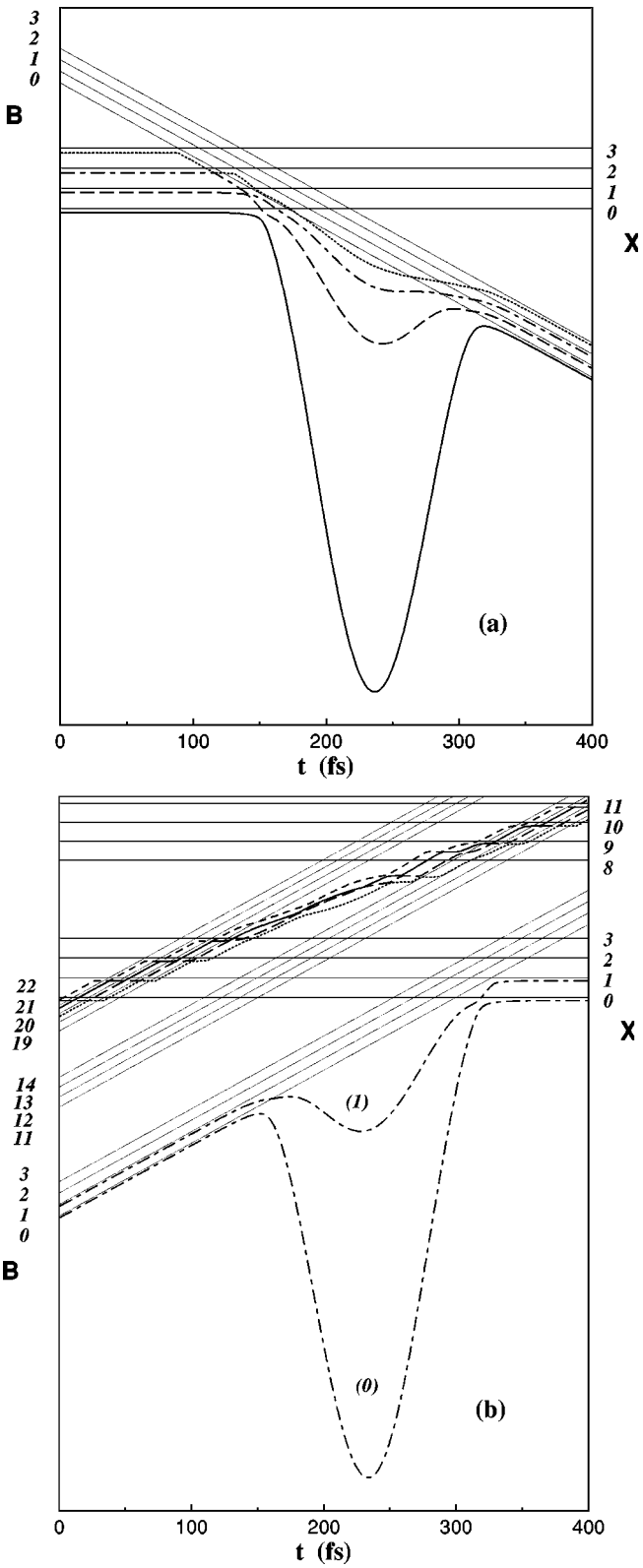

FIG. 7. Schematic of multiple crossings of vibrational levels of the electronic potentials X and B of I_2, when the Rabi frequency is larger then the vibrational energy spacings. In this figure, $\Omega_0 \gg \delta_{X,B}$, and the frequency detuning is -0.012 a.u. (2634 cm^{-1}). Panel (a) illustrates the effects of a positive chirp of $\alpha' = 2 \times 10^{-5}/cm^{-2}$, and panel (b) the effect of a negative chirp of $\alpha' = -2 \times 10^{-5}/cm^{-2}$.

a very complex dressed-state picture consisting of an enormous number of crossings and avoided crossings. However, even in this case the differences between positive and negative chirps can be demonstrated clearly.

Figure 7 shows the dressed potential-energy curves corresponding to the case of population transfer from a ground vibrational manifold to an excited vibrational manifold using strong chirped pulses. Figure 7(a) illustrates the situation for positive chirps, and Fig. 7(b) that for negative chirps. Once again, at early times the population is assumed to be in the state X_0. For positive chirps, as seen in the figure, a direct route exists between population that correlates with X_0 at early times to B_0 at later times. This route is indicated in Fig. 7(a) by a solid line. However, if, at the time of the first avoided crossing between X_0 and B_0, the laser field is not strong enough to maintain adiabaticity, the population can follow alternative routes (long-dashed and dot-dashed lines) as well. These routes correlate to excited vibrational levels of the excited state at later times. Eventually, all of the population is transferred to the excited surface. This mechanism explains the large areas of efficient, robust transfer as a function of the detuning, Rabi frequency and chirp rate in Figs. 3–5.

In the case of a negative chirp, as shown in Fig. 7(b), an extremely different dressed-state picture emerges. In fact, the negative chirp picture is simply the time reverse of the positive chirp, but the population transfer dynamics are quite different. As seen in the figure, the initial population in the X_0 state does not have a direct route to vibrational levels on the B state. Three potentially important routes are shown on the plot by thick solid, dashed, and dotted lines. At later times some of those routes correlate to excited-state vibrational levels, while others correlate to ground-state vibrational levels. The competition among these routes leads to a sensitive dependence of the transfer on the pulse parameters. As a result, while some areas of robust, efficient population transfer for negative chirps do exist, as shown in Figs. 3–5, they are considerably smaller than those for the positive chirp case.

V. CONCLUSIONS

In this paper we analyze the effects of the intensity, chirp rate and frequency detuning on vibronic population transfer. We show, in agreement with the results of CBW [30], that in the case of zero detuning, with fixed bandwidth pulses, positive chirps are more efficient and robust than negative chirps in achieving optimal population transfer. However, with an appropriate choice of frequency detuning, negative chirps can also produce efficient transfer. The regions of robust transfer are in general smaller for negative chirps than for positive chirps, but are nonetheless large enough to be significant for experiments.

To understand the mechanism of population transfer we use a dressed-state picture and a Landau-Zener model of multiple crossings of vibrational levels. Depending on the relative size of the Rabi frequency compared to the vibrational energy spacing, the transfer can be considered to proceed via individual, sequential crossings, or via multiple, nearly simultaneous crossings. The dressed-state model provides a simple framework for understanding population dynamics in which the dominant effects of the laser parameters, time scales, and adiabaticity are treated consistently and with appropriate emphasis.

ACKNOWLEDGMENTS

We thank D. Reitze, K. Schafer, and P. Bucksbaum for helpful and stimulating discussions. This work was partially supported by the National Science Foundation through Grant No. CHE-9875080. This research was supported by an award from Research Corporation.

[1] K. Bergmann and B. W. Shore, in *Molecular Dynamics and Spectroscopy by Stimulated Emission Pumping*, edited by H. L. Dai and R. W. Field (World Scientific, Singapore, 1995), pp. 315–373.
[2] K. Bergmann, H. Theuer, and B. W. Shore, Rev. Mod. Phys. **70**, 1003 (1998).
[3] S. Chelkowski, A. Bandrauk, and P. B. Corkum, Phys. Rev. Lett. **65**, 2355 (1990).
[4] S. Chelkowski and A. D. Bandrauk, Chem. Phys. Lett. **186**, 264 (1991).
[5] F. Legare, S. Chelkowski, and A. D. Bandrauk, J. Raman Spectrosc. **31**, 15 (2000).
[6] J. C. Davis and W. S. Warren, J. Chem. Phys. **110**, 4229 (1999).
[7] J. S. Melinger, S. R. Gandhi, A. Hariharan, D. Goswami, and W. S. Warren, J. Chem. Phys. **101**, 6439 (1994).
[8] P. W. Milonni and J. H. Eberly, *Lasers* (Wiley, New York, 1988).
[9] S. E. Harris, Phys. Rev. Lett. **72**, 52 (1994).
[10] S. E. Harris, Phys. Today **50** (7), 36 (1997).
[11] M. O. Mewes, M. R. Andrews, D. M. Kurn, D. S. Durfee, C. G. Townsend, and W. Ketterle, Phys. Rev. Lett. **78**, 582 (1997).
[12] M. Shapiro and P. Brumer, Int. Rev. Phys. Chem. **13**, 187 (1994).
[13] D. J. Tannor and S. A. Rice, Adv. Chem. Phys. **70**, 441 (1988).
[14] D. Neuhauser and H. Rabitz, Acc. Chem. Res. **26**, 496 (1993).
[15] W. S. Warren, H. Rabitz, and M. Dahleh, Science **259**, 1581 (1993).
[16] R. J. Gordon and S. A. Rice, Annu. Rev. Phys. Chem. **48**, 601 (1997).
[17] J. L. Krause, R. M. Whitnell, K. R. Wilson, and Y. J. Yan, in *Femtosecond Chemistry*, edited by J. Manz and L. Wöste (VCH, Weinheim, 1995), pp. 743–779.
[18] B. W. Shore, *The Theory of Coherent Atomic Excitation* (Wiley, New York, 1990).
[19] L. Allen and J. H. Eberly, *Optical Resonance and Two-Level Atoms* (Dover, New York, 1987).

[20] A. Abragam, *Principles of Nuclear Magnetism* (Oxford University Press, Oxford, 1961).
[21] W. S. Warren, Science **242**, 878 (1988).
[22] M. M. T. Loy, Phys. Rev. Lett. **32**, 814 (1974).
[23] S. Ruhman and R. Kosloff, J. Opt. Soc. Am. B **7**, 1748 (1990).
[24] B. Hartke, R. Kosloff, and S. Ruhman, Chem. Phys. Lett. **158**, 238 (1989).
[25] A. Paloviita, K.-A. Suominen, and S. Stenholm, J. Phys. B **28**, 1463 (1995).
[26] J. S. Melinger, S. R. Gandhi, A. Hariharan, J. X. Tull, and W. S. Warren, Phys. Rev. Lett. **68**, 2000 (1992).
[27] C. J. Bardeen, V. V. Yakovlev, K. R. Wilson, S. D. Carpenter, P. M. Weber, and W. S. Warren, Chem. Phys. Lett. **280**, 151 (1997).
[28] D. J. Maas, D. I. Duncan, R. B. Vrijer, W. J. van der Zande, and L. D. Noordam, Chem. Phys. Lett. **290**, 75 (1998).
[29] D. J. Maas, M. J. J. Vrakking, and L. D. Noordam, Phys. Rev. A **60**, 1351 (1999).
[30] J. Cao, C. J. Bardeen, and K. R. Wilson, Phys. Rev. Lett. **80**, 1406 (1998).
[31] V. V. Yakovlev, C. J. Bardeen, J. Che, J. Cao, and K. R. Wilson, J. Chem. Phys. **108**, 2309 (1998).
[32] C. J. Bardeen, Q. Wang, and C. V. Shank, J. Phys. Chem. A **102**, 2759 (1998).
[33] C. J. Bardeen, V. V. Yakovlev, J. Che, J. A. Squier, and K. R. Wilson, J. Am. Chem. Soc. **120**, 13023 (1998).
[34] M. D. Feit, J. A. Fleck, and A. Steiger, J. Comput. Phys. **47**, 412 (1982).
[35] P. Schwendner, F. Seyl, and R. Schinke, Chem. Phys. **217**, 233 (1997).
[36] C. W. Hillegas, J. X. Tull, D. Goswami, D. Strickland, and W. Warren, Opt. Lett. **19**, 737 (1994).
[37] V. S. Malinovsky and J. L. Krause, Eur. Phys. J. D (to be published).
[38] M. V. Ammosov, N. B. Delone, and V. P. Krainov, Zh. Éksp. Teor. Fiz. **91**, 2008 (1986) [Sov. Phys. JETP **64**, 1191 (1986)].
[39] L. V. Keldysh, Zh. Éksp. Teor. Fiz. **47**, 1945 (1964) [Sov. Phys. JETP **20**, 1307 (1965)].
[40] L. D. Landau, Phys. Z. Sowjetunion **2**, 46 (1932).
[41] C. Zener, Proc. R. Soc. London, Ser. A **137**, 696 (1932).
[42] J. L. Krause, R. M. Whitnell, K. R. Wilson, Y. J. Yan, and S. Mukamel, J. Chem. Phys. **99**, 6562 (1993).